

## Tip-Induced Modification of Polyoxometalate-Dodecane Thiol Self-Assembled Monolayers on Au(111) during Scanning Tunneling Microscopy Imaging

Jandee Kim,<sup>†</sup> Hyeran Kim,<sup>‡,§</sup> Choong Kyun Rhee,<sup>†,‡,\*</sup> Jongwon Kim,<sup>#,\*</sup> and Myung Hwan Whangbo<sup>†</sup>

<sup>†</sup>Department of Chemistry, Chungnam National University, Daejeon 305-764, Korea. \*E-mail: ckrhee@cnu.ac.kr

<sup>‡</sup>Graduate School of Analytical Science and Technology, Chungnam National University, Daejeon 305-764, Korea

<sup>§</sup>Division of Materials Science, Korea Basic Science Institute, Daejeon 305-333, Korea

<sup>#</sup>Department of Chemistry, Chungbuk National University, Cheongju, Chungbuk 361-763, Korea

\*E-mail: jongwonkim@chungbuk.ac.kr

<sup>†</sup>Department of Chemistry, North Carolina State University, Raleigh, NC 27695, USA

Received June 14, 2012, Accepted June 26, 2012

**Key Words :** Au(111), Polyoxometalate, Self-assembled monolayer, Dodecanethiol, Scanning tunneling microscopy

Self-assembled monolayers (SAMs) of thiolates on Au surfaces have been extensively investigated for the last few decades because such systems offer useful applications in the field of nanoscience and nanotechnology.<sup>1</sup> Among the various methods for characterizing the structures of SAMs on Au surfaces, scanning tunneling microscopy (STM) provides unique information about the organization of SAMs at the molecular level.<sup>2</sup> Furthermore, STM has been useful as a lithography tool utilizing tip-induced desorption.<sup>3,4</sup> Specifically, STM tips under very negative tip bias voltages (tip-to-surface electron tunneling) around  $-3$  V remove thiolates underneath them in vacuum<sup>5,6</sup> as well as in nonpolar solvents,<sup>7-9</sup> which allow for further wet etching and replacement with other thiolates, respectively. The tip-induced desorption depends on various experimental parameters such as tip bias voltage, tunneling current, and potential applied at Au substrates.<sup>4</sup> Similarly, the STM tip-induced phase transitions of thiolate-based SAMs on Au<sup>10,11</sup> indicate that STM tips can modify the surface they probe.

In the present work we report on a tip-induced modification of dodecane thiolate (DT,  $\text{CH}_3(\text{CH}_2)_{11}\text{SH}$ ) SAM on Au(111) incorporated with  $\text{SiMo}_{12}\text{O}_{40}^{4-}$ , a polyoxometalate (POM) anion, in 0.1 M  $\text{H}_2\text{SO}_4$  solution (hereafter referred to as POM/DT SAM). POMs constitute a large class of metal oxide molecules with various structures, sizes and chemical reactivities, and are widely utilized in heterogeneous and homogeneous catalysis.<sup>12</sup> In our previous work,<sup>13</sup> it was shown that POM anions adsorbed on the SAM of alkanethiols on Au form a composite organic-inorganic hybrid layer, and that the adsorbed POM anions serve as electron transfer channels for the electrochemically active species such as  $\text{Fe}(\text{CN})_6^{3-}$ ,  $\text{Ru}(\text{NH}_3)_6^{3+}$  and 1,1-ferrocenedimethanol. The specific POM anion plays a role as an electron transfer channel for electrochemistry, but also as a modifier as described here. We observed that the structure of POM/DT SAM during STM scanning was uniquely modified in contrast to the unscanned area. The tip-induced structural changes in DT SAM in the presence and absence of

adsorbed POM were examined, including the effects of scanning conditions and times. A possible mechanism associated with the tip-induced modification of POM/DT SAM was discussed.

Figure 1 shows a series of STM images of POM/DT SAM on Au(111) in 0.1 M  $\text{H}_2\text{SO}_4$  solution under the conditions of various tip bias voltages. Figure 1(a), obtained right after STM tip engagement, displays a surface feature only with DT SAM such as Au vacancy islands. The adsorbed POMs were not visible (see below). As the time elapsed and as the tip bias voltage decreased from  $-185$  mV to  $-280$  mV, extremely small spots arrayed linearly became notable on the terraces as exemplified in the inset of Figure 1(b). At a lower tip bias voltage ( $-515$  mV), relatively large but unidentifiable bright spots ( $0.32 \pm 0.01$  nm) were discernable at the bottom of Figure 1 (c). With a further decrease in the tip bias voltage to  $-550$  mV, the upper terrace in Figure 1(d) became slightly blurred due probably to a movement of adsorbates, whereas the number of large bright spots in the lower terrace increased. In the next image (Fig. 1(e)), the large bright spots disappeared with the advent of a long trench whose depth (approximately 0.23 nm) corresponds to the length of DT (0.24 nm) or one atomic height of Au (0.24 nm). In addition, there was no Au vacancy island near the long trench, and the Au vacancy islands on both terraces became larger due most likely to aggregation of small Au vacancy islands to larger ones. As shown in Figure 1(f), a further decrease in the tip bias voltage ( $-700$  mV) induces relatively wide flat DT layers without any Au vacancy island and simultaneously small domains of lines in the vicinities of the step and trench (See the inset in Figure 1(f)). An increase of the tip bias voltage to  $-530$  mV does not induce any further significant modification, as shown in Figure 1(g), except for the disappearance of the small domains of lines. Figure 1(h), observed 80 min after the image of Figure 1(g) was taken, contrasts the scanned and unscanned areas. The scanned area for Figures 1(a)-(g) lies inside the square, and the outside of the square is scanned for the first time:

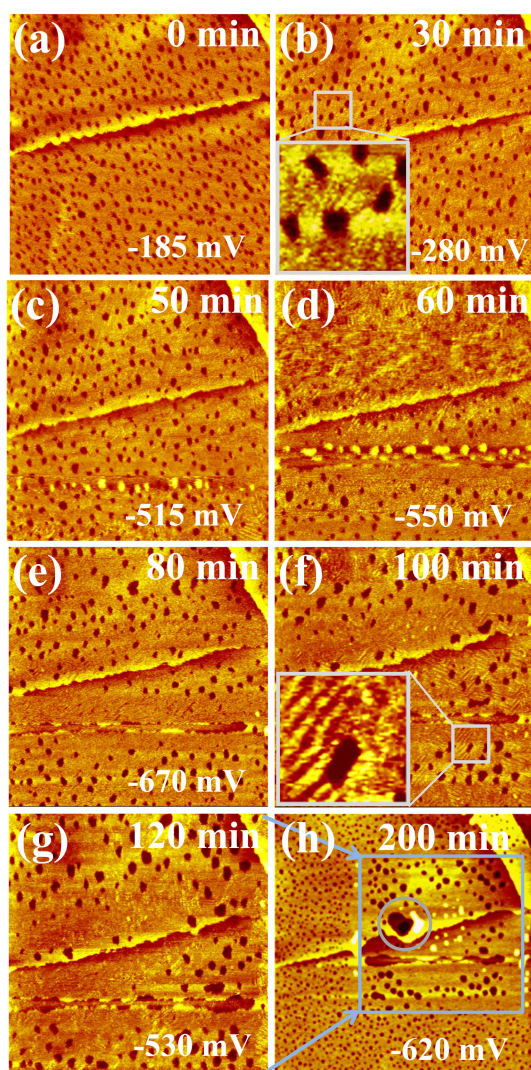


**Figure 1.** Surface modification of POM/DT SAM on Au(111) in 0.1 M  $\text{H}_2\text{SO}_4$  during STM scanning under various tip bias voltages. The times of image acquisition after tip engagement are (a) 0, (b) 30, (c) 50, (d) 60, (e) 80, (f) 100, (g) 120, and (h) 200 min. The insets in (b) and (f) are zoomed images of the squares. Tip bias voltages were specifically indicated in each figure. Tunneling current: (a)-(d) 1.096 nA, (e)-(g) 1.200 nA, (h) 5.326 nA. Image size: (a)-(g)  $200 \times 200 \text{ nm}^2$ , (h)  $350 \times 350 \text{ nm}^2$ .

there was absolutely no modification in the unscanned area. Thus, the modification of POM/DT SAM on Au(111) is clearly induced during the STM scanning.

Figure 2 shows the effect of scanning time on the modification of POM/DT SAM under the STM tip with a fairly constant tip bias voltage around  $-350 \text{ mV}$ . Right after the tip engagement, the POM/DT SAM appears as usual as presented in Figure 1(a). A scanning for 35 min modifies the POM/DT SAMs, *i.e.*, parts of the adsorbed layer on the wide terrace appears to be stripped off, as shown in Figure 2(b). The height difference between the stripped and unstripped parts was  $0.21 \pm 0.02 \text{ nm}$ , approximately corresponding to a length of dodecane thiol ( $0.24 \text{ nm}$ ). In Figure 2(c), the stripped areas expanded with further STM scanning, and

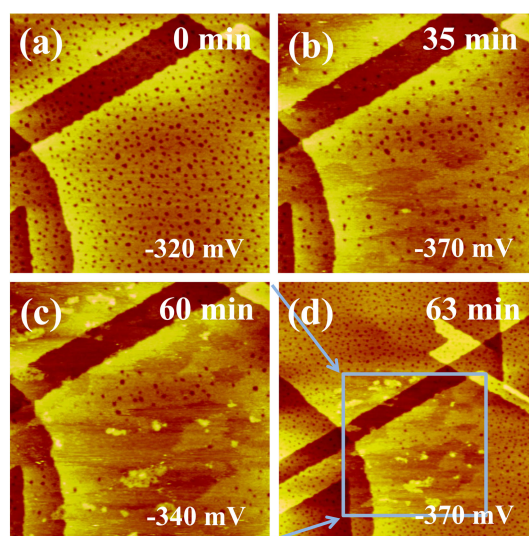
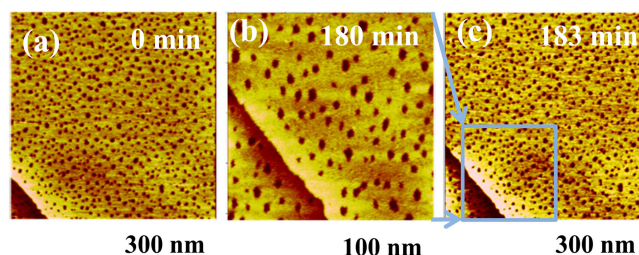


**Figure 2.** Surface modification of POM/DT SAM on Au(111) in 0.1 M  $\text{H}_2\text{SO}_4$  during STM scanning under a fairly constant tip bias voltage ( $-350 \text{ mV}$ ). The times of image acquisition after tip engagement are (a) 0, (b) 35, (c) 60, and (d) 63 min. Tip bias voltages were specifically indicated in each figure. Tunneling current: 0.872 nA. Image size: (a)-(c)  $200 \times 200 \text{ nm}^2$ , (d)  $350 \times 350 \text{ nm}^2$ .

new bright spots of  $0.27 \pm 0.02 \text{ nm}$  in height appear. Zooming out the scanning area (Fig. 2(d)) confirms that only the scanned area of POM/DT SAM for 1 hr was modified. Though not shown, similar modifications are observed on thiolate SAMs of octane and octadecane on Au(111) with adsorbed POM.

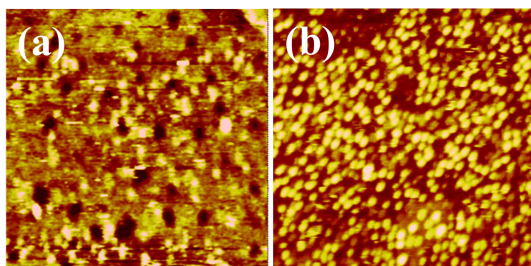
Figure 3 shows STM images of DT SAM on Au(111) without adsorbed POMs. The image obtained right after the tip engagement (Fig. 3(a)) is typical of alkylthiolate SAM on Au(111). After scanning with tip bias voltage of  $-1.0 \text{ V}$  for 3 hr (Fig. 3(b)), however, there occurs no modification on POM/DT SAMs as demonstrated in Figure 3(c). Consequently, it is the presence of POM on DT SAM that causes the modification of POM/DT SAMs on Au(111) during the STM scanning.

Figure 4 compares the STM images of POM on Au(111) acquired with tip bias voltage of  $-1.0$  and  $-0.9 \text{ V}$  in the presence and absence of DT SAM. There are clearly dis-



**Figure 3.** STM images of DT SAM on Au(111) in 0.1 M  $\text{H}_2\text{SO}_4$  as scanning time elapsed. The times of image acquisition after tip engagement are (a) 0, (b) 180, and (c) 183 min. Tip bias voltage:  $-1.0 \text{ V}$ . Tunneling current: 1.240 nA. Image size: (a) and (c)  $300 \times 300 \text{ nm}^2$ , (b)  $100 \times 100 \text{ nm}^2$ .





**Figure 4.** STM images of POM on Au(111) (a) with and (b) without DT SAM in 0.1 M H<sub>2</sub>SO<sub>4</sub>. Tip bias voltage: (a)  $-1.0$  and (b)  $-0.9$  V. Tunneling current: (a) 1.200 and (b) 1.960 nA. Image size:  $50 \times 50$  nm<sup>2</sup>.

cernible bright spots ( $0.5 \pm 0.1$  nm in height) corresponding to the adsorbed POM (see below). The presence of POM on the investigated POM/DT SAMs on Au(111) was confirmed in our previous study<sup>13</sup> by X-ray photoelectron spectroscopy (XPS) and voltammetric measurements. Specifically, the XPS measurements showed the Mo and S peaks arising from POMs and DTs, respectively. In addition, the adsorbed POMs made it possible for the species of Fe(CN)<sub>6</sub><sup>3-</sup>, Ru(NH<sub>3</sub>)<sub>6</sub><sup>3+</sup> and 1,1-ferrocenedimethanol to undergo electrochemical redox reactions with POMs acting as electron channels in the inert DT SAM. The amount of the adsorbed POM on the surface, estimated with three different techniques (*i.e.*, XPS, voltammetry and STM), is consistently in the range of 20–30%.

It is worthwhile to discuss in some detail the presence of POMs in POM/DT SAMs on Au(111) in conjunction with the STM observations. The spots corresponding to POMs in DT SAM are observable right after the tip engagement with bias of  $-1.0$  V, as shown in Figure 4(a). However, a tip bias voltage higher than  $-1.0$  V (*e.g.*,  $-0.7$  V as in Fig. 1) always leads to STM images displaying only DT SAMs with Au vacancy islands, implying that the electron tunneling through POM (lying above DT SAM) is less efficient than that through DT. The adsorbed POMs on DT SAM may make the tip-to-surface path poorly conductive for electron tunneling. In fact, the POMs on Au(111) without DT SAM were clearly visible at the tip bias voltage of  $-0.9$  V (Fig. 4(b)). During the STM scanning, the STM tip may press down the POMs into the SAM layer towards the Au(111) surface until the set-point current is reached. The extent of tip-to-surface electron tunneling is governed by the tip bias voltage and the set-point current, as revealed by the variation in the height of the STM spots of POMs:  $0.27 \pm 0.02$  nm at  $-0.34$  V with set current of 0.872 nA (Fig. 2(c)),  $0.32 \pm 0.01$  nm at  $-0.7$  V with set current of 1.096 nA (Fig. 1(c)), and  $0.5 \pm 0.1$  nm at  $-1.0$  V with set current of 1.200 nA (Fig. 4(a)). With a tip bias voltage of  $-1.0$  V or even more negative ones, the feedback loop of the employed STM instrument becomes too unstable to keep the STM tip engaged to the POM/DT SAM surface. This makes it difficult to acquire a series of STM images for a significant period of time.

In conclusion, the surface of POM/DT SAMs on Au(111)

is significantly modified by STM scanning, indicating that the POMs lying above SAMs make the tip-to-surface path very poorly conductive for electron tunneling. This makes the tip approach the surface closer to achieve the set current, and the concomitant mechanical interaction of the tip with the POM/DT SAM lying underneath forces the dodecane thiolates and Au atoms to move, resulting in the desorption of dodecane thiolates from the Au surface.

## Experimental

The (111) facet of Au bead, prepared by melting a Au wire (0.5 mm diameter, Aldrich, 99.999%) in a hydrogen-oxygen flame, was used for our STM experiments. The adsorption of dodecanethiol on the Au(111) surface was carried out by contacting the Au single crystal bead with an ethanolic solution of 1 mM dodecanethiol (CH<sub>3</sub>(CH<sub>2</sub>)<sub>11</sub>SH, Aldrich, 98%) for 12 h. The subsequent modification of the DT SAM with POM was performed by dipping the DT SAM on Au(111) into a solution of 1 mM POM (SiMo<sub>12</sub>O<sub>40</sub><sup>4-</sup>, Aldrich, 98%) + 0.1 M H<sub>2</sub>SO<sub>4</sub> (Merck, suprapur) for 12 h. STM experiments were performed in 0.05 M H<sub>2</sub>SO<sub>4</sub> solution with Nanoscope IIIa (Digital Instrument) equipped with a tungsten tip (0.25 mm diameter, Aldrich, 99.9%), made by electrochemical etching and coating with a polyethylene melt, and a home-made liquid cell.

**Acknowledgments.** This work was supported by Basic Research Program (2010-0007527) and Specialized Graduate School Program (2009-008146) through NRF grant funded by the MEST. CKR appreciates the financial support of Chungnam National University for his stay at North Carolina State University (USA).

## References

- Love, J. C.; Estroff, L. A.; Kriebel, J. K.; Nuzzo, R. G.; Whitesides, G. M. *Chem. Rev.* **2005**, *105*, 1103.
- Alves, C. A.; Smith, E. L.; Porter, M. D. *J. Am. Chem. Soc.* **1992**, *114*, 1222.
- Smith, R. K.; Lewis, P. A.; Weiss, P. S. *Prog. Surf. Sci.* **2004**, *75*, 1.
- Yang, G.; Liu, G.-Y. *J. Phys. Chem. B* **2003**, *107*, 8746.
- Lercel, M. J.; Redinbo, G. F.; Pardo, F. D.; Rooks, M.; Tiberio, R. C.; Simpson, P.; Craighead, H. G.; Sheen, C. W.; Parikh, A. N.; Allara, D. L. *J. Vac. Sci. Technol. B* **1994**, *12*, 3663.
- Kleineberg, U.; Brechling, A.; Sundermann, M.; Heinzmann, U. *Adv. Funct. Mater.* **2001**, *11*, 208.
- Gorman, C. B.; Carroll, R. L.; He, Y. F.; Tian, F.; Fuierer, R. *Langmuir* **2000**, *16*, 6312.
- Gorman, C. B.; Carroll, R. L.; Fuierer, R. *Langmuir* **2001**, *17*, 6923.
- Fuierer, R.; Carroll, R. L.; Feldheim, D. L.; Gorman, C. B. *Adv. Mater.* **2002**, *14*, 154.
- Seo, K.; Borguet, E. *J. Phys. Chem. C* **2007**, *111*, 6335.
- Lee, J. S.; Chi, Y. S.; Kim, J.; Yun, W. S.; Choi, I. S. *Phys. Chem. Chem. Phys.* **2008**, *10*, 3138.
- Katsoulis, D. E. *Chem. Rev.* **1998**, *98*, 359.
- Chu, Y.; Kim, J.; Choi, S.; Rhee, C. K.; Kim, J. *Appl. Surf. Sci.* **2011**, *257*, 9490.